PERGAMON

International Journal of Multiphase Flow 27 (2001) 2023–2041

International Journal of Multiphase Flow

www.elsevier.com/locate/ijmulflow

Enhancement of shock waves in a porous medium saturated with a liquid containing soluble-gas bubbles

V.E. Dontsov *, V.E. Nakoryakov

Institute of Thermophysics SB RAS, 630090, Novosibirsk, Russia

Received 16 April 2000; received in revised form 3 July 2001

Abstract

Evolution of a moderate-intensity shock wave and its enhancement after reflection from a rigid surface embedded in a porous medium are studied experimentally. The medium is saturated with a liquid that has bubbles of a soluble gas. A physical mechanism of shock wave enhancement in a saturated porous medium is proposed. Experimental data on the amplitude and velocity of reflected waves are compared with results of theoretical modeling. The process of gas bubble dissolution behind a shock wave is studied. © 2001 Elsevier Science Ltd. All rights reserved.

Keywords: Porous medium; Liquid; Gas bubbles; Shock wave; Enhancement; Dissolution

1. Introduction

Kedrinsky (1980) numerically calculated collapse of bubbles in a cavitation layer near a solid wall. He discovered of a series of high-amplitude pressure impulses on the wall, which was caused by the inertia effect of collective bubble collapse. Lauterborn and Vogel (1984) and Tomita and Shima (1990) registered by optical methods a powerful secondary shock wave, which developed after a single bubble collapsed in the liquid. Shima and Fujiwara (1992) investigated the effect of interaction of close bubbles on their destruction and generation of secondary shock waves. Borisov et al. (1982), Nakoryakov et al. (1983), Tepper (1983), Pokusaev et al. (1991), and Dontsov (1998) experimentally proved that shock wave enhancement may take place in a liquid with vapor bubbles (or in a liquid with readily soluble gas bubbles). This kind of enhancement may occur in a direct wave or in a wave reflected from a solid surface.

* Corresponding author.

PII: S0301-9322(01)00049-0

Theoretical and experimental studies of evolution, structure, and reflection from a solid wall of a pressure perturbation in a liquid suspension of solid particles and gas bubbles were performed by Nakoryakov et al. (1996) and Dontsov and Pokusaev (1999). Shreiber (1997) developed a model for penetration of nonlinear acoustic waves in a three-phase mixture. The waves' evolution equations were derived and used for explanation of some experimental data on wavy dynamics in a three-phase medium. Theofanous et al. (1998) and Hanratty et al. (1998) considered the effects of phase interaction in multiphase disperse systems, including phase transitions and chemical reactions. Stability of phase boundaries in a multiphase medium and dynamics of solid and gaseous inclusions were also considered.

Nakoryakov et al. (1989) and Dontsov (1992) studied the evolution and structure of weakly nonlinear pressure waves in a porous medium saturated with a liquid or a liquid with gas bubbles. The existence of two kinds of longitudinal waves (''fast'' and ''slow'' modes) was proven; both are caused by the difference in compressibility of the porous skeleton and the filling liquid.

This paper is devoted to experimental study of evolution of a moderate-intensity shock wave propagation in a porous medium saturated with a liquid and bubbles of a soluble gas and its enhancement after reflection from a rigid surface. A mechanism of wave enhancement in a saturated porous medium was proposed. We compare experimental data with calculations based on models developed by Lyakhov (1982) and Nigmatulin (1990). The process of gas bubble dissolution behind a shock wave is also investigated.

2. Theoretical analysis

2.1. Adiabatic model

Let us consider reflection of a 1D shock wave from a solid wall in a saturated porous medium using an adiabatic model developed by Lyakhov (1982). Lyakhov's model for nonlinear liquid multicomponent medium without viscosity gives us the following formulas for velocities of incident and reflected shock waves:

$$U_0 = ((P_1 - P_0)/\rho_0(1 - \phi_0\varepsilon_0(P_1/P_0)^{-1/\gamma} - (1 - \varepsilon_0)\phi_0(\gamma^*(P_1 - P_0)/(\rho_{20}c_2^2) + 1)^{-1/\gamma^*} - (1 - \phi_0)(\gamma^{**}(P_1 - P_0)/(\rho_{10}c_1^2) + 1)^{-1/\gamma^{**}})^{-1})^{0.5}, \quad (1)$$

$$U_1 = ((P_2 - P_1)/\rho_1(1 - \phi_1\varepsilon_1(P_2/P_1)^{-1/\gamma} - (1 - \varepsilon_1)\phi_1(\gamma^*(P_2 - P_1)/(\rho_{20}c_2^2) + 1)^{-1/\gamma^*} - (1 - \phi_1)(\gamma^{**}(P_2 - P_1)(\rho_{10}c_1^2) + 1)^{-1/\gamma^{**}})^{-1})^{0.5}, \quad (2)$$

$$\rho_0 = \rho_{10}(1 - \phi_0) + \rho_{20}\phi_0(1 - \varepsilon_0) + \rho_{30}\phi_0\varepsilon_0, \quad (3)$$

$$\rho_1 = \rho_{10}(1 - \phi_1) + \rho_{20}\phi_1(1 - \varepsilon_1) + \rho_{30}\phi_1\varepsilon_1. \quad (4)$$

Here U_1 is the velocity of the reflected wave relative to the medium ahead of the wave; ρ_0, ρ_1 are the densities of the three-phase medium ahead of and behind the front of the incident shock wave, ρ_{10}, ρ_{20}, ρ_{30} are the densities of the solid, liquid and gaseous phases ahead of the front of the shock wave; ϕ_0, ϕ_1 are the porosities of the three-phase mixture ahead of and behind the wave front; ε_0, ε_1 are the volumetric void fractions ahead of and behind the wave front, hence $\phi_0\varepsilon_0$, $\phi_1\varepsilon_1$ are the void fractions ahead of and behind the wave front in the three-phase medium; γ, γ^*, γ^{**} are the

adiabatic indices for the gaseous, liquid, and solid phases, respectively; P_0, P_1, P_2 are the pressures ahead of the wave incident on the wall, behind the front, and behind the reflected wave front, respectively; c_1, c_2 are the sound velocities in the solid and liquid phases. Note that this model accounts for the compressibility of the material of the porous medium, but disregards the elasticity of the porous skeleton.

If we assume that the solid and liquid phase are incompressible and the behavior of the gas in bubbles is adiabatic, then the void fraction and porosity behind the shock wave front are described by the following formulas:

$$\varepsilon_1 = \varepsilon_0((1-\varepsilon_0)(P_1/P_0)^{1/\gamma} + \varepsilon_0)^{-1}, \tag{5}$$

$$\phi_1 = \phi_0(1-\varepsilon_0)/((1-\varepsilon_1) + \phi_0(\varepsilon_1 - \varepsilon_0)). \tag{6}$$

According to the effective viscosity approximation used for description of stationary shock waves, the condition for the reflection of a stationary shock wave from a solid wall in a three-phase medium can be written in the form (Nigmatulin, 1990)

$$(P_1 - P_0)/(\rho_0 U_0) = (P_2 - P_1)/(\rho_1 U_1). \tag{7}$$

Correspondingly, the velocity of the reflected shock wave relative to the wall takes the form proposed by Nigmatulin (1990):

$$U_2 = U_1 - (P_1 - P_0)/(\rho_0 U_0). \tag{8}$$

Formulas (1)–(8) allow us to calculate the amplitude and velocity of a shock wave reflected from a solid wall in a three-phase medium for the adiabatic approximation.

The adiabatic model assumes that the gas bubbles behind a shock wave are adiabatic, i.e., heat transfer from the gas to the surrounding liquid medium is neglected. The reflection of the shock wave from the rigid surface is governed by adiabatic law, when the time of thermal relaxation τ_t of the gas in bubbles (Nigmatulin, 1990) is much longer than the time of the shock wave's front propagation τ_f (Table 1). The time of front propagation relative to any measurement point means

Table 1

The thermal relaxation time for gas in bubbles	$\tau_t = R_0^2/\pi^2 a_0$	At $R_0 \approx 50 \times 10^{-6}$ m, $\tau_t \sim 10^{-5}$ s At $R_0 \approx 250 \times 10^{-6}$ m, $\tau_t \sim 6 \times 10^{-4}$ s
The time of shock wave's front propagation	τ_f	$(10\text{–}100) \times 10^{-6}$ s
The time of the shock wave	t	$(1\text{–}10) \times 10^{-3}$ s
The gas bubble collapse time for a stepwise pressure variation due to diffusion	$\tau_d = \dfrac{R_0^2}{(2D_1(\varepsilon_R - \varepsilon_\infty))}$	At $P_0 = 0.1$ MPa, $P_1/P_0 = 10$, $R_0 \approx 50 \times 10^{-6}$ m, $\tau_d \sim 1$ s
The time of equalizing for the velocities of gas and liquid phases behind a shock wave	$\tau_\mu = R_0^2/18\nu$	At $R_0 \approx 50 \times 10^{-6}$ m, $\tau_\mu \sim 10^{-4}$ s At $R_0 \approx 250 \times 10^{-6}$ m, $\tau_\mu \sim 10^{-3}$ s
The time of equalizing for the velocities of solid and liquid phases behind a shock wave	$\tau_{\mu d} = \dfrac{d^2\rho_{10}}{72\nu\rho_{20}}$	At $d = 3 \times 10^{-3}$ m, $\tau_{\mu d} = 0.1$ s
The gas bubble collapse time for a stepwise pressure variation due to convective diffusion	$\tau_c = \dfrac{1.5\sqrt{\pi/2}R_0^{3/2}}{(\varepsilon_R - \varepsilon_\infty)(D_1 V)^{0.5}}$	At $R_0 \approx 250 \times 10^{-6}$ m, $P_0 = 0.1$ MPa, $\tau_c \sim 10^{-3}$ s

there the time of pressure growth from initial pressure ahead of the wave to its averaged pressure. To study the reflected shock wave velocity (2), the condition $\tau_t \gg t^*$ must be fulfilled. Here t^* is the time of the incident shock wave passing up to the moment of arrival of the reflected shock wave at the measurement point.

2.2. Equilibrium model

Let us consider the reflection of shock waves from a solid wall in a three-phase medium using an equilibrium model for evolution of waves in a gas–liquid medium (Nigmatulin, 1990). With the elasticity of the porous skeleton disregarded, a liquid containing solid particles has the following effective density and low-frequency sound velocity (Wood's formula, see Nakoryakov et al., 1996; Johnson and Plona, 1982):

$$\rho_{m0} = (\rho_{10}(1-\phi_0) + \rho_{20}\phi_0(1-\varepsilon_0))/(1-\phi_0\varepsilon_0), \tag{9}$$

$$c_m = ((1-\phi_0)/(c_1^2\rho_{10}) + \phi_0/(c_2^2\rho_{20}))^{-0.5}(\rho_{10}(1-\phi_0) + \rho_{20}\phi_0)^{-0.5}. \tag{10}$$

The incident and reflected shock wave velocities for this model have the following respective forms:

$$U_0 = \left(\frac{P_1}{\rho_{m0}(1-\phi_0\varepsilon_0)\phi_0\varepsilon_0}\,\frac{1+(P_1/P_0-1)P_0/(c_m^2\rho_{m0})}{1+(P_1/P_0-\phi_0\varepsilon_0)P_0/(c_m^2\phi_0\varepsilon_0\rho_{m0})}\right)^{0.5}, \tag{11}$$

$$U_1 = \left(\frac{P_2}{\rho_{m1}(1-\phi_1\varepsilon_1)\phi_1\varepsilon_1}\,\frac{1+(P_2/P_1-1)P_1/(c_{m1}^2\rho_{m1})}{1+(P_2/P_1-\phi_1\varepsilon_1)P_1/(c_{m1}^2\phi_1\varepsilon_1\rho_{m1})}\right)^{0.5}, \tag{12}$$

$$\rho_{m1} = (\rho_{10}(1-\phi_1) + \rho_{20}\phi_1(1-\varepsilon_1))/(1-\phi_1\varepsilon_1), \tag{13}$$

$$c_{m1} = ((1-\phi_1)/(c_1^2\rho_{10}) + \phi_1/(c_2^2\rho_{20}))^{-0.5}(\rho_{10}(1-\phi_1) + \rho_{20}\phi_1)^{-0.5}. \tag{14}$$

Formulas (9)–(14) jointly with (5)–(8), wherein $\gamma = 1$, provide the amplitude and velocity for a shock wave reflected from a solid wall in a three-phase medium (the isothermal approximation).

According to the isothermal model, the temperatures of the gas and liquid immediately behind the front of the shock wave are equal. This assumption is valid at τ_t much less than the duration τ_f of the front of the incident shock wave. However, for wave amplitudes $P_1/P_0 \gg 1$ the adiabatic (1) and isothermal (11) velocities of shock waves are rather close. The main difference between these models is in the determination of the volumetric gas void fraction behind the shock wave (5), i.e., whether adiabatic or isothermal ($\gamma = 1$) compression of bubbles takes place in the shock wave. Then for wave amplitudes $P_1/P_0 \gg 1$ the validity of the isothermal model can be expanded up to the condition $\tau_t \ll t^*$.

2.3. Isothermal model with complete gas dissolving

Using the equilibrium model and formula for velocity of the pressure jump in a vapor–liquid mixture with complete vapor condensation behind the shock wave's front (Nigmatulin, 1990), we obtain a law for the reflection of a shock wave from a solid wall in a three-phase medium with gas dissolution. We use the assumption of complete gas dissolution behind the incident wave. Hence, the reflected wave penetrates through a liquid with solid particles without gas bubbles. In this

case, as for a two-phase medium, a considerable amplification of the reflected shock wave takes place. The expression for its amplitude is as follows:

$$P_2/P_1 = 1 + \left(c_{\mathrm{m}}^2 \phi_0 \varepsilon_0 \rho_{\mathrm{m}0}(1-\phi_0\varepsilon_0)(\rho_{10}(1-\phi_1)+\rho_{20}\phi_1)^2/(\rho_0^2 P_1)\right)^{0.5}(1-P_0/P_1)^{0.5}. \quad (15)$$

The model for shock wave reflection from a solid wall assumes that a complete dissolution takes place behind the incident shock wave and its velocity is equal to the value prevailing when the condensation takes place (Nigmatulin, 1990).

3. Experimental setup

Our experiments were performed in a shock tube (see the diagram in Fig. 1). The working section (1) was a vertical thick-walled iron tube with an inner diameter of 0.053 m and a length of 1 m, bounded by a solid wall (2) at the bottom. The working section was filled with a porous

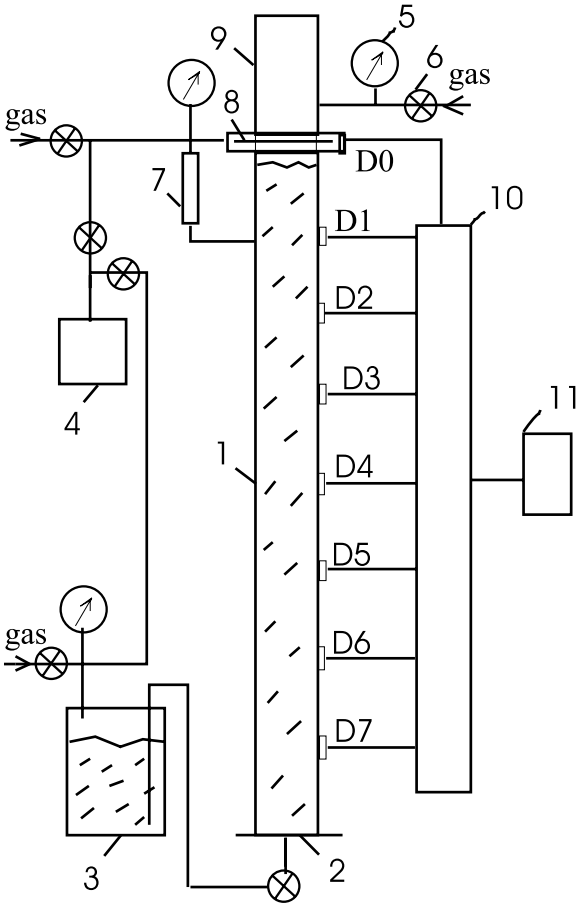

Fig. 1. Diagram of experimental setup.

medium. This was a random bed of polyethylene particles with a size of 3.5 mm (porosity $\phi_0 = 0.37$) or foam rubber ($\phi_0 = 0.98$). Distilled water was the working liquid and air (or carbon dioxide) was the gas phase. The solubility coefficients of air in water and carbon dioxide are essentially different. The preparation of the medium was as follows. The porous medium, saturated with the gas, was in the working section under pressure P_0. The gas-saturated liquid (at equilibrium state) was in tank 3 at pressure $(P_0 + \Delta P_0)$. Then the porous medium under pressure P_0 was filled with the liquid from tank 3. The liquid filled all the pores, and the initial gas void fraction was $\varepsilon_0 = 0$. After the static pressure P_0 was reduced to the atmospheric level, the gas was released from the liquid, and the initial gas void fraction ε_0 was established in the medium. The uniformity of distribution of ε_0 over the section length was controlled by the velocity of the incident shock wave. As for the distribution of ε_0 over the tube cross-section, it was assumed to be uniform and was not measured.

After the propagation of the shock wave, the medium lost some gas content and the initial parameters were slightly changed. But after the propagation of a strong shock wave, the degassing and nonuniformity of ε_0 distribution became significant and we stopped experimenting with this medium. To control the supply of gas and liquid, vacuum pump (4), pressure gauges (5) and valves (6) were used.

Direct measurements of bubble size were difficult because the porous medium was nontransparent. The bubble size was estimated in the following way. If we consider the nucleation of gas bubbles to be a heterogeneous process, which is valid for regular distilled water, one can estimate the critical radius of a nucleus when the bubble begins growing (Nigmatulin, 1990): $a_* = 2\sigma/\Delta P_s$. Here σ is the coefficient of the liquid surface tension, ΔP_s is the static pressure drop. For preparation of a porous medium filled with water with air bubbles, $\Delta P_s \geqslant 0.2$ MPa and the size of the critical nucleus was estimated as $a_* \leqslant 10^{-6}$ m. We can also estimate the radius of the bubble developed from a nucleus at the time of pressure release. For bubbles of air and for the range of void fraction studied, this radius is $R_0 \approx 50 \times 10^{-6}$ m. We assumed that the number of critical nuclei with a typical size of $a \approx 10^{-6}$ m per unit volume of water is $n \approx 10^{12}$ m^{-3} (Nigmatulin, 1990).

We prepared a porous medium filled with bubbly water (carbon dioxide); the pressure release was $\Delta P_s \approx 0.02$ MPa. This gave us the following critical size of a nucleus: $a_* \approx 10^{-5}$ m. Since the size of the critical nucleus is by one order of magnitude higher than the air bubble size, the number of nucleation sites for carbon dioxide will be much less. Correspondingly, after static pressure release, the size of developed carbon dioxide bubbles will be much greater than that of the air bubbles at the same void fraction. Some measurements of the half-height of a solitary wave in a porous medium filled with water and carbon dioxide bubbles (Nakoryakov et al., 1996) give us the bubble radius $R_0 \sim 250 \times 10^{-6}$ m.

Varying the value of ΔP_s, one changes the initial void fraction ε_0 in the liquid. The value of the void fraction in the porous medium averaged over the working section was determined by measuring the change in the height of the liquid in the measurement duct (7) after a decrease in the initial static pressure in the medium.

Stepwise pressure waves were started by disrupting the diaphragm (8), which separated the high-pressure chamber (9) and the working section. Profiles of pressure waves were recorded by piezoelectric pressure probes D1–D7 positioned along the length of the working section. Here D0 is a triggering probe for ADC (10). The pressure probes did not touch the skeleton of the porous

medium and measured the pressure in the liquid phase. Signals from these probes were supplied to the ADC and then processed in the computer (11).

Fig. 2 presents typical profiles of pressure shock waves at different distances X from the inlet of a saturated porous medium (the parameters of the medium are shown in Table 2). One can

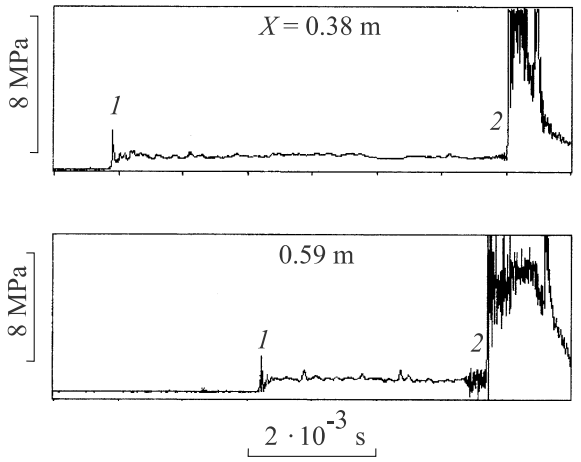

Fig. 2. Profiles of pressure waves in a foam rubber filled with water and air bubbles. $P_1/P_0 = 10.9$.

Table 2

Figure (N)	Experiment or calculation	Nature of gas	ϕ_0	ε_0	P_0 (MPa)
Fig. 2	Exp.	Air	0.98	0.18	0.104
Fig. 3	Exp. – 1; cal. – 4, 7	Air	0.98	0.18	0.104
	Exp. – 2; cal. – 5, 8	Air	0.98	0.19	0.056
	Exp. – 3; cal. – 6, 9	Carbon dioxide	0.98	0.105	0.104
Fig. 4	Exp. – 1; cal. – 3, 5	Air	0.98	0.18	0.104
	Exp. – 2; cal. – 4, 6	Air	0.98	0.19	0.056
	Cal. – 7	Air	0.98	0.14	0.056
	Exp. – 8; cal. – 9, 10	Carbon dioxide	0.98	0.105	0.104
Fig. 5	Exp. – 1; cal. – 3, 5	Air	0.37	0.105	0.103
	Exp. – 2; cal. – 4, 6	Air	0.37	0.095	0.203
	Exp. – 7; cal. – 9	Carbon dioxide	0.37	0.05	0.103
	Exp. – 8; cal. – 10	Carbon dioxide	0.37	0.10	0.103
Fig. 6	Exp. – 1; cal. – 3	Air	0.98	0.18	0.104
	Exp. – 2; cal. – 4	Air	0.98	0.19	0.056
	Cal. – 5	Air	0.98	0.14	0.056
	Exp. – 6; cal. – 7	Carbon dioxide	0.98	0.105	0.104
Fig. 7	Exp. – 1; cal. – 2	Air	0.37	0.105	0.103
	Exp. – 3; cal. – 5	Carbon dioxide	0.37	0.05	0.103
	Exp. – 4; cal. – 6	Carbon dioxide	0.37	0.10	0.103
Fig. 8	Exp.	Air	0.37	0.05	0.10
Fig. 9(a)	Cal. – 1, 2, 3	Air	0.98	0.18	0.104
	Cal. – 4	Air	0.98	0.114	0.104
	Cal. – 5	Air	0.37	0.105	0.103
Fig. 9(b)	Cal. – 1, 2, 3	Carbon dioxide	0.98	0.105	0.104
	Cal. – 4	Carbon dioxide	0.37	0.10	0.103

see that the incident wave 1 and the reflected wave 2 retain their stepwise shape. For rather high amplitudes $P_1/P_0 \geqslant 10$, one can observe significant pressure pulsations at the front of the shock wave, which are caused by very nonlinear oscillations of bubbles. While spreading, the incident shock wave holds its amplitude and velocity (within the measurement accuracy). The reflected shock wave is not a stationary one, because it spreads through a medium with a variable gas void fraction. However, for a short path Δx, when the wave velocity changes insignificantly at a distance of about a wavelength, we can consider the reflected shock wave as quasistationary.

The amplitude of a shock wave was measured from the average value of the pressure behind its front. The velocity of a shock wave was determined from the difference between the time of arrival of the wave front to two neighboring probes and the distance between them.

4. Experimental results

4.1. Dynamics of a shock wave

Due to the experimental study of evolution of shock waves with a moderate amplitude in a saturated porous medium, it has been shown that the initial signal penetrating into the porous medium separates into "fast" and "slow" modes. These modes are caused by the difference in the compressibility of the porous skeleton and the gas–liquid mixture that saturates this skeleton (Dontsov, 1992). The "slow" wave quickly attenuates because of friction at the liquid–solid interface. The "fast" wave almost holds its stepwise shape. In our experiments we studied the evolution of a "fast" pressure wave and its reflection from a solid wall; therefore, the term "fast" will be skipped below.

The shock wave velocity U_0 in foam rubber saturated with bubbly water versus the wave amplitude P_1/P_0 is shown in Fig. 3 for various medium parameters. Here P_0 is the pressure ahead of the shock wave, P_1 is the pressure behind the shock wave front, and 1–3 are experimental points for various values of the initial volumetric void fraction ε_0 and P_0 in the medium (Table 2). Lines 4–6 represent calculations by the adiabatic model (1)–(8), and lines 7–9 represent calculations by the isothermal model (5)–(14). In the calculations, the gas dissolution behind the wave was not considered. For air bubbles $\gamma = 1.4$, for carbon dioxide $\gamma = 1.3$, and for water $\gamma^* = 7$. It is obvious that the experimental data are within the range lying between the adiabatic and isothermal approximations for corresponding medium parameters. This is caused by the fact that the time of thermal relaxation τ_t for the gas in bubbles is close to the duration of the front of the shock wave, especially for air bubbles with radius $R_0 \approx 50 \times 10^{-6}$ m (Table 1). a_0 is the coefficient of thermal conductivity in bubbles. For air bubbles at $P_0 = 0.1$ MPa $a_0 = 2.2 \times 10^{-5}$ m^2/s, and for carbon dioxide $a_0 = 10^{-5}$ m^2/s. The duration of the incident and reflected shock wave in our experiments varied from $\sim$10 up to hundreds of microseconds (depending on the wave amplitude).

Besides, a tendency to an increase in the shock wave velocity with the wave amplitude P_1/P_0 was observed in the experiments in comparison with the calculated values: points 2 are lines 5 and 8, and points 3 are lines 6 and 9. This is caused by a decrease in the initial volumetric void fraction in the medium after propagation of a shock wave. That is, after propagation of a shock wave

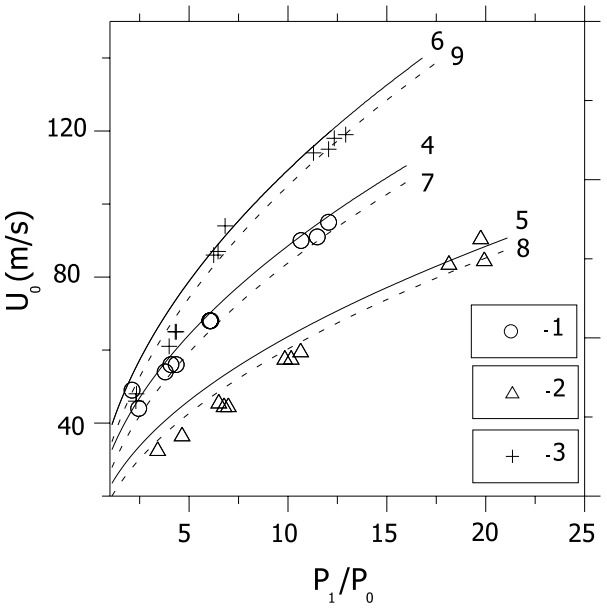

Fig. 3. Shock wave velocity.

through a medium (especially a shock wave with a high amplitude), some portion of the gas leaves the porous medium, and ε_0 changes (decreases).

4.2. Shock wave's reflection. Air bubbles case

Points 1 and 2 in Fig. 4 demonstrate some experimental data for the reflected shock wave amplitude P_2 in a porous medium: foam rubber saturated with water and air bubbles of relatively small size: $R_0 \approx 50 \times 10^{-6}$ m (the parameters of the medium are in Table 2). The porous skeleton, due to its low rigidity and great porosity, does not significantly affect the shock wave reflection from a solid wall. It only holds the gas bubbles in the liquid. Lines 3 and 4 show calculations by the adiabatic model (1)–(8), and lines 5–7 demonstrate calculations by the isothermal model (5)–(14). It is obvious that experimental data 1 and 2 are in agreement with the isothermal approximation 5 and 6 for the corresponding medium parameters. For high amplitudes, however, experimental points 2 deviate from calculated values 6, which is caused by a decrease in the initial volumetric void fraction for waves with higher amplitudes (line 7) (notice that the value $\varepsilon_0 = 0.14$ was obtained by direct measurement of the initial gas void after the passing of strong shock waves with an amplitude P_1/P_0 of $\sim$20). Besides, at higher wave amplitudes, the law of wave's reflection from a solid wall is nearly the adiabatic law due to a decrease in the time of the incident shock wave front. This time becomes less than the time of thermal relaxation of gas in bubbles. Points 1 tend to adiabatic calculation 3 for wave amplitudes $P_1/P_0 \geqslant 10$. Therefore, the process of gas dissolution in the liquid behind the shock wave is weak and has no significant effect on the law of reflection from a solid wall.

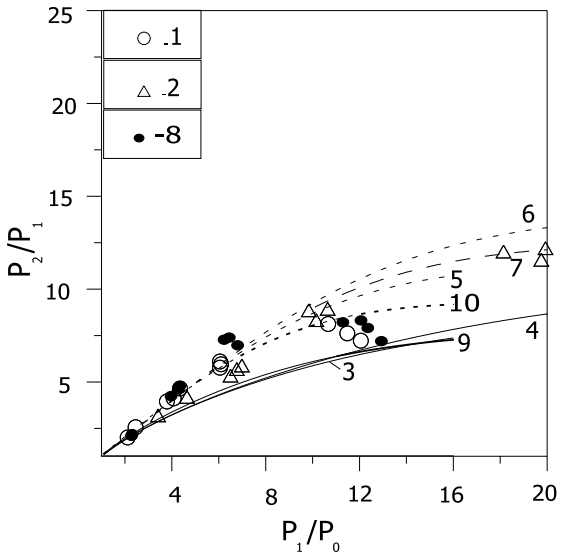

Fig. 4. Amplitude of a shock wave reflected from a rigid wall in a foam rubber filled with water and gas bubbles.

Some experiments performed for a lower initial gas void fraction ($\varepsilon_0 \sim 0.1$) revealed that an increase in ε_0 does not affect the gas dissolving in a high-porosity medium and, correspondingly, the reflection law from a solid wall.

However, the pattern changes qualitatively, when shock waves reflect from a solid wall in a porous medium of tightly coupled polyethylene particles. In Fig. 5 points 1 and 2 show some experimental data for the amplitude of a reflected shock wave in a dense porous medium saturated with water and air bubbles (the parameters of the medium are in Table 2). Lines 3 and 4 correspond to calculation by the isothermal model (5)–(14), and lines 5 and 6 demonstrate calculations for the reflection of a shock wave with complete condensation (dissolution) from a solid wall (15). In the calculations for the dense porous medium, we used the following value of low-frequency sound velocity, experimentally measured in a saturated porous medium without gas bubbles: $c_m = 1590$ m/s, we took $\gamma^{**} = 4$, and $\rho_{10} = 920$ kg/m^3.

Above a certain wave amplitude P_1/P_0, one can observe a significant amplification of shock waves (points 1 and 2) in comparison with calculations (3, 4), done by the isothermal model. The latter did not account for the process of gas dissolution in the liquid behind the wave. Hence, the dense porous medium provides for intensive gas dissolution behind the shock wave, thereby facilitating amplification of the reflected shock wave. This amplification is caused by transition of the kinetic energy of radial liquid motion at bubble collapse into the potential energy of pressure in the liquid (Kedrinsky, 1980; Borisov et al., 1982; Dontsov, 1998). The contribution of inertia forces into enhancement of a shock wave in a gas–liquid mixture was calculated by Nigmatulin (1990) for a specific example. He demonstrated that the inertia forces of a bubble collapsing in a shock wave amplified the wave considerably. To amplify shock waves, it is necessary that the gas dissolution caused by diffusion processes take place in a time close to the duration of the front of the shock wave.

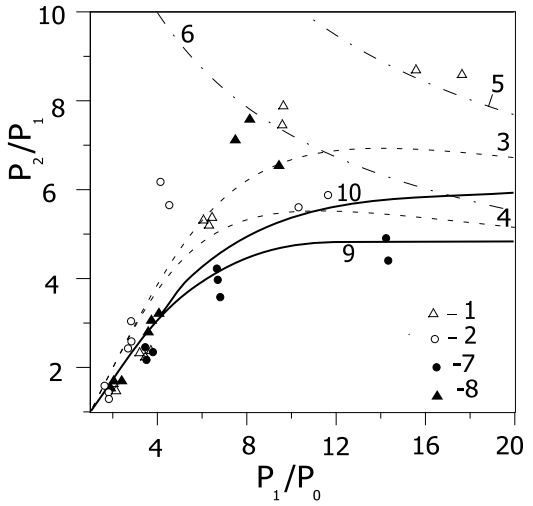

Fig. 5. Amplitude of a shock wave reflected from a rigid wall in a dense porous medium filled with water and gas bubbles.

Notice that the process of shock wave amplification is not caused by bubble splitting behind the shock wave, like it was observed during wave evolution in a liquid with large bubbles (Dontsov, 1998; Dontsov and Pokusaev, 1999). The Weber number (We), which determines instability and splitting of bubbles in a shock wave (Nigmatulin, 1990), in our experiments is significantly less than its critical value ($We = (\rho_{30} R_0 V^2)/\sigma \ll We^* \sim 2\pi$). Here V is the relative velocity of gas bubbles in the liquid behind the wave, $V \sim (P_1 - P_0)/(\rho_0 U_0)$ (Nigmatulin, 1990).

One can see from comparison of experimental data 1 and 2 that an increase in the initial static pressure P_0 leads to amplification of the reflected shock wave amplitude (points 2) in comparison with calculated values (lines 4) at lower wave amplitudes P_1/P_0. This is caused by a decrease in the bubble radius with a rise of P_0, and, consequently, by an increase in the area of interface at a constant value of ε_0. Besides, an increase in P_0 leads to a higher concentration of dissolved gas on the bubble surface, and, consequently, to an increase in the rate of gas dissolution in the liquid. As the wave amplitude P_1/P_0 increases, the experimental data 1 and 2 approach the corresponding curves 5 and 6 calculated by accounting for complete gas dissolution in the liquid behind the incident shock wave.

Points 1 and 2 in Fig. 6 show the experimental velocity U_2 of the shock wave reflected from a solid wall in foam rubber saturated with water and air bubbles versus the amplitude of the incident shock wave P_1/P_0 (the parameters of the medium are shown in Table 2). The measurements of the velocity of the reflected shock wave shown in all figures were performed in a certain section Δx of the shock tube located near the top of the working section. Lines 3 and 4 demonstrate calculations by the isothermal model (5)–(14). It is obvious that experimental data 1 and 2 are in agreement with isothermal approximation 3 and 4, which does not consider the process of gas dissolution behind the incident wave, for the corresponding parameters of the medium. For high wave amplitudes, however, points 2 deviate from calculated values 4. This is caused by a decrease in the initial volumetric void fraction for waves with high amplitude (line 5). Hence, the process of

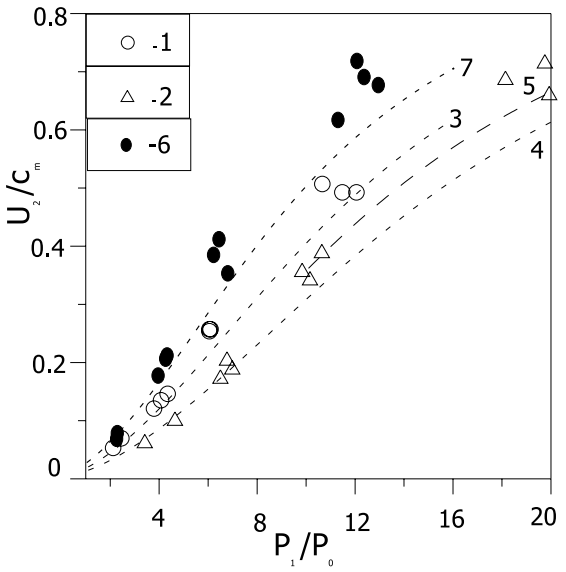

Fig. 6. Velocity of reflected shock wave in a foam rubber filled with water and gas bubbles.

gas dissolution in the liquid behind the incident wave in a medium where the influence of the porous skeleton can be neglected is insignificant and does not lead to any increase in the velocity of the reflected shock wave.

Let us obtain estimates confirming the result obtained above. An estimate obtained for the gas bubble collapse time τ_d at a stepwise pressure jump caused by diffusion shows that the dissolution process behind the shock during a time period $t \sim 10$ ms and for a bubble radius decrease $R/R_0 = (1 - t/\tau_d)^{0.5}$ is insignificant (Epstein and Plesset, 1950, see also Table 1). For instance, at $P_1/P_0 = 10$, $P_0 = 0.1$ MPa, the collapse time $\tau_d \sim 1$ s. D_1 is the coefficient of gas diffusion in the liquid, ε_R, ε_∞ are the volumetric concentrations of the gas dissolved in the liquid at the boundary of a bubble and far from it, respectively. For air at room temperature and $P_0 = 0.1$ MPa, $D_1 = 2 \times 10^{-9}$ m^2/s, and $\varepsilon_\infty = 0.02$. Convective mass transfer due to relative motion of air bubbles in water is also insignificant (Nigmatulin, 1990) because the time τ_μ of phase velocity relaxation is of the order of dozens of microseconds (Table 1).

Points 1 in Fig. 7 show experimental velocity values of a shock wave reflected from a solid wall in a close-packed saturated porous medium (the parameters of the medium are in Table 2). Line 2 corresponds to calculation by the isothermal model (5)–(14). It is clear that, with a rise of the wave amplitude, experimental values 1 of the reflected shock wave velocity deviate from calculation curve 2. Hence, the gas dissolves in the liquid behind the incident wave. This process leads to reduction of the initial volumetric void fraction behind the wave, and, consequently, to an increase in the velocity of the reflected shock wave. For wave amplitudes $P_1/P_0 > 10$, the experimental values of the reflected shock wave velocity significantly deviate from the results of calculation. That is, the process of gas dissolution mainly determines the gas behavior behind the shock wave. For the propagation of shock waves in three-phase suspensions with relatively large bubbles (Dontsov and Pokusaev, 1999), the process of gas dissolution in the liquid behind a shock

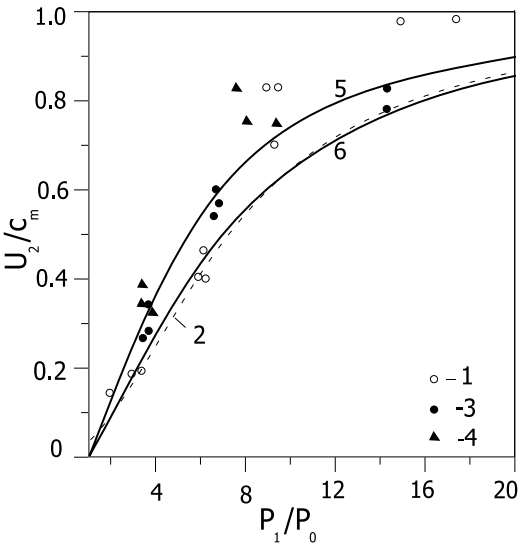

Fig. 7. Velocity of a reflected shock wave in a dense porous medium filled with water and gas bubbles.

wave is caused by bubble splitting. In these experiments, the intensive mass transfer occurring behind the shock wave in a dense porous medium is apparently caused by the turbulent movement of the liquid in that region.

Let us present some estimates confirming the turbulent movement of the liquid behind the shock wave. Actually, the Reynolds number determined by the diameter d of solid particles in a porous medium and the relative velocity W of liquid and solid phases behind the shock wave is $Re_d = dW/v \gg 100$. Here v is the kinematic viscosity of the liquid. Therefore, the regime of liquid flow in a porous medium has a turbulent character (Jolls and Hanratty, 1996). An estimate of the relative velocity W was obtained using calculations by the model of Biot (Nakoryakov et al., 1989). Notice that the time of equalizing $\tau_{\mu d}$ for the velocities of solid and liquid phases behind a shock wave (Nigmatulin, 1990) caused by interphase friction is significantly higher than the time of the shock wave propagation (Table 1).

For high wave amplitudes in a porous medium filled with gas bubbles and a liquid with a developed interface, amplification of a shock wave takes place not only after reflection from a solid wall, but also behind the front of the incident shock wave. Typical structures of a shock wave with high amplitude are shown in Fig. 8 at different distances X from the inlet of the porous medium (the parameters of the medium are shown in Table 2). These structures formed from an initial signal of a stepwise shape. With propagation of shock wave *1* through the medium, pressure impulse *2* of high amplitude is formed behind the wave front. The impulse velocity is close to the velocity of the front of the shock wave, and its amplitude reaches the amplitude of reflected shock wave *3*. The formation of the powerful pressure impulse behind the shock wave front is caused by pressure pulsation in the liquid at collapse of gas bubbles due to their intensive dissolution. Mass transfer intensification by turbulent motion of the liquid behind the wave leads to wave amplification even in a medium with bubbles of air, which is weakly soluble in water. As for reflected shock waves, amplification of an incident wave is of a

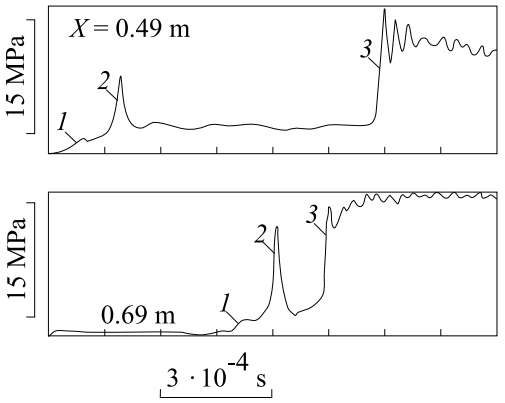

Fig. 8. Evolution of a shock wave with a high amplitude through a porous medium filled with water and air bubbles. $P_1/P_0 = 28$.

threshold nature. If the amplitude of a shock wave rises to a level when gas dissolution takes place during a period close to the duration of the wave front, a dissolution wave develops. The effects of porosity and other important parameters of the porous medium on wave amplification are not considered in this paper.

The process of shock wave amplification in liquids with bubbles of a readily soluble gas and in a vapor–liquid medium was observed by Borisov et al. (1982) and Pokusaev et al. (1991).

4.3. Shock wave's reflection. Carbon dioxide bubbles case

Let us consider reflection of a shock wave from a solid wall in a porous medium saturated with water and bubbles of a readily soluble gas, namely, carbon dioxide. The amplitude P_2 of the shock wave reflected from a solid wall in foam rubber saturated with water and carbon dioxide bubbles versus the amplitude P_1/P_0 of the incident shock wave is shown in Fig. 4 (see also Table 2). Points 8 demonstrate experimental data; line 9 shows calculation according to the adiabatic model (1)–(8), and line 10 shows calculation by the isothermal model (5)–(14). For experimental points 8, the time of thermal relaxation of gas in bubbles is $\tau_t \sim 0.6$ ms, that is considerably longer than the duration of the reflected shock wave front. Therefore, the law of shock wave reflection from a solid wall is expected to be close to adiabatic. However, in the experiments we observe amplification of the reflected shock wave in comparison with calculations 9. As for the case of air bubbles, the effect of amplification of the reflected shock wave is not caused by bubble splitting in the wave ($We \leqslant We^*$). Intensive mass transfer, caused by amplification of the reflected wave, can stem from convective diffusion assisted by relative bubble movement in the liquid behind the shock wave.

Below we present estimates confirming this assumption. Using a relation for the mass transfer coefficient of a gas bubble floating up in a liquid, obtained under the approximation of the diffusion boundary layer (Wijngaarden, 1967; Kutateladze and Nakoryakov, 1984), the resulting expression for the mass transfer coefficient per unit surface of a bubble due to its relative motion in the liquid behind the shock wave is as follows: $\beta_c = (2D_1V/\pi R)^{0.5}$. The time of collapse for gas

bubbles for a stepwise pressure variation in the wave due to convective diffusion is τ_c (Table 1). The bubble radius decreases as $R/R_0 = (1 - t/\tau_c)^{2/3}$. Assuming that the number of bubbles per unit volume of the medium is constant, we obtain an expression for the real mass transfer coefficient per unit surface of a bubble behind the shock wave: $\beta_t = (d\varepsilon^*/dt)R/(3(\varepsilon_R - \varepsilon_\infty))$. Here ε^* is the relative value of dissolved gas behind the shock wave. For a shock wave amplitude $P_1/P_0 = 12$ in foam rubber saturated with water and carbon dioxide bubbles, the estimated ratio of the real mass transfer coefficient behind the shock wave to the convective mass transfer coefficient at the initial stage of bubble collapse is as follows: $\beta_t/\beta_c \sim 1$. Hence, convective diffusion caused by relative motion of gas bubbles in the liquid makes a major contribution to the mass transfer behind the shock wave. Notice that in the calculations the velocity of relative motion of a gas bubble V was assumed to be equal to the liquid velocity behind the wave. However, this is true only for $t \ll \tau_\mu$.

Reduction of the amplification effect of reflected waves at amplitudes of $P_1/P_0 \geqslant 10$ is caused by a decrease in the initial volumetric void fraction for a strong shock wave (some bubbles leave the porous medium after the strong shock wave has passed). The calculation curve that takes into account complete dissolution of the gas behind the incident shock wave is significantly higher than the experimental values. This testifies that gas dissolution behind the shock wave is relatively moderate.

Points 7 and 8 in Fig. 5 show some experimental data on the amplitudes of a shock wave reflected from a solid wall in a dense porous medium saturated with water and carbon dioxide bubbles, for various values of the initial volumetric void fraction in the liquid (Table 2). Lines 9 and 10 show calculation by the adiabatic model (1)–(8). It is obvious that for an initial volumetric void fraction $\varepsilon_0 = 0.05$, experimental data 7 coincide with calculation curve 9 (which does not account for gas dissolution behind the wave). With an increase in the initial volumetric void fraction ($\varepsilon_0 = 0.10$), the mass transfer processes behind the wave enhance the reflected shock wave.

Fig. 6 shows some experimental data 6 for the velocity U_2 of a shock wave reflected from a solid wall in foam rubber, saturated with water and bubbles of readily soluble carbon dioxide versus the amplitude of the incident shock wave (Table 2). Line 7 demonstrates calculation by the isothermal model (5)–(14). It is clear that with a rise of the wave amplitude P_1/P_0, the experimental velocity values 6 of the reflected shock wave deviate from calculation curve 7. Therefore, the gas dissolves in the liquid behind the incident shock wave. This process leads to a decrease in the initial volumetric void fraction behind the wave, i.e., to an increase in the velocity of the reflected shock wave. The process of gas dissolution behind the shock wave is caused by convective diffusion due to the relative motion of gas bubbles in the liquid behind the wave.

Experimental data 3 and 4 on the velocity U_2 of a reflected shock wave in a dense porous medium filled with water and bubbles of readily soluble carbon dioxide versus the amplitude of the incident shock wave are shown in Fig. 7 (see also Table 2). Lines 5 and 6 demonstrate calculations carried out by the isothermal approximation (5)–(14) for the corresponding values of the initial volumetric void fraction. It is obvious that for an initial volumetric void fraction $\varepsilon_0 = 0.05$, experimental values of shock wave velocity 3 perfectly coincide with the calculated curve 5, i.e., the process of gas dissolution in the liquid behind the wave can be neglected. With an increase in ε_0, the dissolution process becomes considerable, and experimental points 4 deviate from calculation curve 6.

From the above comparison of Figs. 4 and 5, as well as Figs. 6 and 7, we conclude that the influence of the porous medium porosity on the process of carbon dioxide dissolution is small.

4.4. Gas dissolution after the impact of a shock wave

Let us consider the process of gas dissolution in the liquid behind an incident shock wave in a saturated porous medium using measurements for the reflected wave amplitude and velocity. Using the experimental values for the reflected wave amplitude and velocity in the calculation model (5)–(14), we can determine the volumetric void fraction ε_1^* behind the incident shock wave taking into account gas dissolution in the liquid. Measuring the velocity of the reflected shock wave in some separate regions of its propagation, we can determine ε_1^* for the gas phase behind the front of the incident shock wave as a function of high pressure exposition time. Correspondingly, we can calculate the relative void fraction of the dissolved gas behind the shock wave: $\varepsilon^* = (\varepsilon_1 - \varepsilon_1^*)/\varepsilon_1$; here ε_1 is the calculated volumetric void fraction behind the shock wave without allowance for gas dissolution at $\gamma = 1$ (5).

The dots in Fig. 9 show calculation of the relative void fraction of the gas dissolved in water behind an incident wave in a saturated porous medium versus the pressure exposition time t of gas

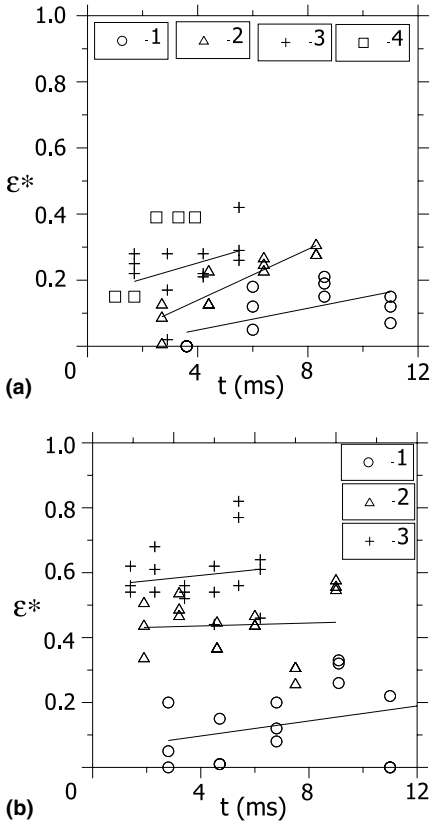

Fig. 9. Relative void fraction of the dissolved gas behind the shock wave. (a) 1 – $P_1/P_0 = 4.0$; 2 – $P_1/P_0 = 6.0$; 3 – $P_1/P_0 = 12.0$; 4 – $P_1/P_0 = 24.0$. (b) 1 – $P_1/P_0 = 4.0$; 2 – $P_1/P_0 = 6.0$; 3 – $P_1/P_0 = 12.0$.

phase behind the wave front for various medium and wave parameters (Table 2). The solid lines are averaged calculation values for the parameters P_1/P_0 and ε_0. The calculation was performed using experimental values of the reflected wave amplitude and velocity measured in some separate regions of wave propagation. The relatively wide scatter in the data may be due to measurement errors produced by the numerous parameters used in the calculations (P_1/P_0, ε_0, U_2, P_2), and by nonuniformity of ε_0 distribution along the working section.

It is obvious that in a wide range of wave amplitudes P_1/P_0 the relative value of air dissolved in water depends only slightly on the wave amplitude and time, and it exceeds only slightly the measurement error (Fig. 9(a)). An increase in ε^* with a rise of P_1/P_0 may be caused by a decrease in the initial volumetric void fraction of waves with high amplitudes due to the fact that some part of the bubbles leave the porous medium after the shock wave propagation. Nonuniformity of distribution of bubbles along the working section can lead to a weak dependence of ε^* on the time t. Thus, for foam rubber saturated with water and air bubbles, diffusion process during times t of $\sim$10 ms does not lead to a considerable change in the volumetric void fraction behind the shock wave.

It is well known that gas solubility in a liquid depends considerably on the temperature of the medium. However, gas heating in the bubbles of a shock wave presumably does not affect gas solubility. During bubble collapse, heat transfer between the gas and the liquid is controlled by gas parameters, and the temperature of the bubble interface is almost equal to the liquid temperature; it varies only slightly during wave propagation due to the fact that the thermal capacity and thermal conductivity of the liquid are higher then those of the gas. Therefore, the temperature in the diffusion layer outside the bubble varies only slightly. Therefore, it is insignificant for gas solubility. Besides, the greatest temperature change takes place at the final stage of bubble collapse. This time is much less than the typical time of dissolution.

Some calculations of the relative value of air dissolved in water behind a shock wave in a dense porous medium (calculation 5 in Table 2) have demonstrated that for time $t = 1$–2 ms and $P_1/P_0 = 9.2$ we obtain $\varepsilon^* \approx 0.6$, and for $P_1/P_0 = 16.5$ we obtain $\varepsilon^* \approx 0.95$. That is, in a dense porous medium a drastic enhancement of mass transfer at the gas–liquid interface occurs, and with a rise of wave amplitude, the process of gas dissolution in the liquid becomes more intensive.

Using a relation for the mass transfer coefficient of diffusive bubble dissolution in the boundary layer approximation: $\beta_d = D_1/R$ (Epstein and Plesset, 1950; Kutateladze and Nakoryakov, 1984), we obtain the coefficient of mass transfer enhancement caused by a dense porous medium: $\beta_t/\beta_d = (d\varepsilon^*/dt)R^2/(3D_1(\varepsilon_R - \varepsilon_\infty))$. For a wave amplitude $P_1/P_0 = 16.5$ at the initial stage of bubble collapse ($R \sim R_0$), we estimate that $\beta_t/\beta_d \sim 100$. Such a strong enhancement of mass transfer may be caused by turbulent velocity pulsations of the liquid behind a shock wave in a porous medium.

Some calculations of the relative value of carbon dioxide dissolved in water behind a shock wave in saturated foam rubber are shown in Fig. 9(b). It is obvious that, with a rise of the wave amplitude, the process of gas dissolution becomes intensive, and the values calculated for ε^* exceed the calculation error. Some calculations of the relative value of carbon dioxide dissolved in water behind a shock wave in a dense porous medium (calculation 4 in Table 2) have shown that for $t = 1$–2 ms and $P_1/P_0 = 8.2$, we obtain $\varepsilon^* \approx 0.6$. It is clear that ε^* calculated for a porous medium with $\phi_0 = 0.37$ and $\phi_0 = 0.98$ are close to each other at the same wave parameters. Therefore, in the experiments with bubbles of carbon dioxide, ϕ_0 of the porous medium has no

significant effect on the process of gas dissolution in the liquid behind a shock wave, and diffusion due to turbulent motion of the liquid behind the shock wave is not a major mechanism of mass transfer.

We estimate the collapse time for carbon dioxide bubbles behind a shock wave due to convective diffusion at the same parameter values as follows: $\tau_c \sim 1$ ms (Table 1). The time of equalizing the velocities of carbon dioxide bubbles and liquid behind the shock wave is the same: $\tau_\mu \sim 1$ ms (Table 1). Therefore, we can assert that the gas dissolution (see data in Fig. 9(b)) may be caused by convective diffusion due to relative motion of gas bubbles in the liquid behind the shock wave. The weak time dependence of ε^* in Fig. 9(b) (points 2 and 3) at $t > \tau_\mu \sim 1$ ms also indirectly proves the existence of convective mass transfer behind the shock wave.

5. Conclusions

1. Evolution of shock waves after reflection from a solid wall in a porous medium saturated with bubbly water was investigated. Enhancement of a shock wave caused by accelerating collapse of gas bubbles behind the wave front was studied experimentally. It has been shown that, for a relatively small bubble radius ($R_0 \sim 50 \times 10^{-6}$ m), amplification of the reflected shock wave may take place in a medium with bubbles of air, which is slightly soluble in the water. Experimental results on the shock wave reflection were compared with calculations by mathematical models.
2. It has been shown that diffusion greatly intensified by liquid turbulent motion behind a shock wave may be the major mechanism of mass transfer in a porous medium saturated with a liquid having small gas bubbles.
3. For relatively large gas bubbles with relative motion in the liquid, but without bubble splitting, it has been shown that convective diffusion is the major mechanism of mass transfer behind a shock wave.

Acknowledgements

The work has received financial support from the Russian Foundation for Fundamental Research (Grant N 00-01-00831 and Grant N 00-15-96177).

References

Borisov, A.A., Gelfand, B.E., Nigmatulin, R.I., Rakhmatulin, Kh.A., Timofeev, E.I., 1982. Enhancement of shock waves in liquids with vapor- and dissolving gas bubbles. Dokl. Akad. Nauk USSR 263, 594–598.

Dontsov, V.E., 1992. Structure and dynamics of pressure disturbances of final amplitude in a porous medium, saturated by a liquid with gas bubbles. Izv. Akad. Nauk USSR 1, 80–85.

Dontsov, V.E., 1998. Reflection of pressure waves of moderate intensity from a rigid wall in liquid with readily soluble gas bubbles. J. Appl. Mech. Tech. Phys. USSR 5, 19–24.

Dontsov, V.E., Pokusaev, B.G., 1999. Shock wave reflection from a rigid wall in a liquid suspension of solid particles and gas bubbles. Acoust. Phys. 45, 182–189.

Epstein, P.S., Plesset, M.S., 1950. On the stability of gas bubbles in liquid–gas solutions. J. Chem. Phys. 18, 1505–1509.
Hanratty, T.J., Iliopoulos, I., Woods, B., 1998. The roles of interfacial stability and particle dynamics in multiphase flow. In: Book of Abstracts of the Third International Conference on Multiphase Flow, Lyon, France, pp. 0.1-3.
Johnson, D.L., Plona, T.S., 1982. Slow waves and the consolidation transition. J. Acoust. Soc. Am. 72, 556–565.
Jolls, K.R., Hanratty, T.J., 1996. Transition to turbulence for flow through a dumped bed of spheres. Chem. Eng. Sci. 21, 1185–1190.
Kedrinsky, V.K., 1980. Shock waves in a liquid containing gas bubbles. Combust. Explos. Shock Waves USSR 16, 495–504.
Kutateladze, S.S., Nakoryakov, V.E., 1984. Heat Mass Transfer and Waves in Gas–Liquid System. Nauka, Novosibirsk, Russia.
Lauterborn, W., Vogel, A., 1984. Modern optical techniques in fluid mechanics. Annu. Rev. Fluid Mech. 16, 223–244.
Lyakhov, G.M., 1982. Waves in Grounds and Porous Multicomponent Media. Nauka, Moskow, Russia.
Nakoryakov, V.E., Dontsov, V.E., Pokusaev, B.G., 1996. Pressure waves in a liquid suspension with solid particles and gas bubbles. Int. J. Multiphase Flow 22, 417–429.
Nakoryakov, V.E., Kuznetsov, V.V., Dontsov, V.E., 1989. Pressure waves in saturated porous media. Int. J. Multiphase Flow 15, 857–875.
Nakoryakov, V.E., Pokusaev, B.G., Schreiber, I.R., 1983. Propagation of Waves in Gas– and Vapor–Liquid Media. Institute of Thermophysics, Novosibirsk, Russia.
Nigmatulin, R.I., 1990. Dynamics of Multiphase Media. Hemisphere, New York.
Pokusaev, B.G., Pribaturin, N.A., Vasserman, E.S., 1991. Moderate shock wave propagation in vapor–liquid slug flow. In: Proceedings of the 18th International Symposium SWST, Japan, pp. 62–65.
Shima, A., Fujiwara, T., 1992. The behavior of two bubbles near a solid wall. Arch. Appl. Mech. 62, 53–61.
Shreiber, I.R., 1997. Bulk viscidity model in acoustic of bubble water saturated soil. Acustica 83, 430–435.
Tepper, W., 1983. Experimental investigation of the propagation of shock waves in bubbly liquid–vapor mixtures. In: Proceedings of the 14th International Symposium on Shock Tubes and Shock Waves, Australia, pp. 397–404.
Theofanous, T.G., Yuen, W.W., Angelini, S., 1998. The internal dynamic structures of a class of transient dispersed flow with phase change. In: Book of Abstracts of the Third International Conference on Multiphase Flow, Lyon, France, pp. 3.6-1.
Tomita, Y., Shima, A., 1990. High-speed photographic observations of laser induced cavitation bubbles in water. Acustica 71, 161–171.
Van Wijngaarden, L., 1967. On the growth of small cavitation bubbles by convective diffusion. Int. J. Heat Mass Transfer 10, 127–134.